Volume 54(10): 1105–1113, 2006
Journal of Histochemistry & Cytochemistry
http://www.jhc.org

ARTICLE

Localization of Perlecan and Heparanase in Hertwig's Epithelial Root Sheath During Root Formation in Mouse Molars

Azumi Hirata and Hiroaki Nakamura

Department of Oral Morphology, Okayama University Graduate School of Medicine, Dentistry, and Pharmaceutical Sciences, Okayama, Japan (AH), and Department of Oral Histology, Matsumoto Dental University, Shiojiri, Japan (HN)

SUMMARY During cementogenesis, dental follicular cells penetrate the ruptured Hertwig's epithelial root sheath (HERS) and differentiate into cementoblasts. Mechanisms involved in basement membrane degradation during this process have not been clarified. Perlecan, a heparan sulfate (HS) proteoglycan, is a component of all basement membranes. Degradation of HS of perlecan by heparanase cleavage affects a variety of biological processes. We elucidated immunolocalization of perlecan and heparanase in developing murine molars to clarify their roles in cementoblast differentiation. At the initial stage of root formation, perlecan immunoreactivity was detected on the basement membrane of HERS. Weak heparanase immunoreactivity was detected in HERS cells. HERS showed intense staining for heparanase as root formation progressed. In contrast, labeling for perlecan disappeared from the basement membrane facing the dental follicle, and weak immunoreactivity for perlecan was detected on the inner side of the basement membrane of HERS. These findings suggest that perlecan removal is an important step for root and periodontal tissue formation. Heparanase secreted by the cells of HERS may contribute to root formation by degrading perlecan in the dental basement membrane. **(J Histochem Cytochem 54:1105–1113, 2006)**

KEY WORDS
Hertwig's epithelial root sheath
basement membrane
murine model
heparanase
perlecan
root formation
cementogenesis

TOOTH MORPHOGENESIS is regulated by signal molecules such as transforming growth factor β (TGFβ), fibroblast growth factor (FGF), and members of the Hedgehog and Wnt families (Thesleff 2003). These signals mediate cell communication between epithelial and mesenchymal cells, namely, epithelial–mesenchymal interactions. After tooth crown formation, Hertwig's epithelial root sheath (HERS) formed by inner and outer enamel epithelium induces tooth root and periodontal tissue formation. However, the origin of cementoblast is controversial (Bosshardt and Schroeder 1996). According to the classic theory, periodontal tissues are formed by the mesenchymal cells in the dental follicle. In cementogenesis, dental follicle cells penetrate the ruptured HERS and differentiate into cementoblasts. Another possibility is that HERS cells undergo an epithelial–mesenchymal transformation and become functional cementoblasts (Bosshardt and Nanci 1998a; Lezot et al. 2000).

Formation of a mineralized tissue adjacent to the developing root dentin surface is suggested to be dependent on the presence of native components from the basement membrane such as laminin, type IV collagen, and sulfated glycoconjugates (Andujar et al. 1985; MacNeil and Thomas 1993; Tomazela-Herndl and Arana-Chavez 2001,2004). Perlecan is a heparan sulfate proteoglycan (HSPG) present in most basement membranes (Hassell et al. 1980) as well as in the extracellular matrix (Iozzo et al. 1994). Perlecan is believed to play a role in cell growth and differentiation and tissue organization (Iozzo et al. 1994) because cleavage of perlecan leads to release of bioactive agents such as growth factors, cytokines, chemokines, lipoproteins, and enzymes from the glycosaminoglycan side chains (Gallagher 2001; Vlodavsky and Friedmann 2001). Recently, heparanase, an endoglucuronidase, was identified as a key enzyme in the cleavage of the heparan sulfate (HS) chain in perlecan (Hulett et al. 1999; Toyoshima and Nakajima 1999; Vlodavsky et al. 1999). Degradation of HS by heparanase enables cell movement through extracellular barriers and releases

Correspondence to: Azumi Hirata, Department of Oral Morphology, Okayama University Graduate School of Medicine, Dentistry, and Pharmaceutical Sciences, 5-1 Shikata-cho, 2-chome, Okayama 700-8525, Japan. E-mail: yamagata@md.okayama-u.ac.jp

Received for publication November 15, 2005; accepted May 26, 2006 [DOI: 10.1369/jhc.5A6883.2006].

0022-1554/06/$3.30

growth factors from extracellular matrix, making them bioavailable (Parish et al. 2001; Vlodavsky et al. 2002). Heparanase is expressed by epithelial cells, endothelial cells, and activated cells of the immune system in various pathological conditions, as well as in normal development (Vlodavsky et al. 2002).

Several studies have suggested that HSPG present in the basement membrane of the tooth germ plays an important role in tooth development (Thesleff et al. 1981; Laurie et al. 1982). In addition, perlecan immunolocalization in the murine tooth germ has been previously demonstrated on the basement membrane and in the intercellular spaces of the enamel organ, as well as in dental mesenchymal tissues (Ida-Yonemochi et al. 2005). However, there are no published studies on the relationship between perlecan and heparanase during tooth development. The aim of the present study was to determine the immunolocalization pattern of perlecan and heparanase in the developing murine molar to clarify their roles in root formation.

Materials and Methods

All animal studies were in accordance with the Guidelines for Animal Experiments, Okayama University Graduate School of Medicine, Dentistry, and Pharmaceutical Sciences, Okayama, Japan.

Antibody Against Heparanase

A cysteine-conjugated peptide corresponding to residues 28–45 (DDVVDLEFYTKRPLRSVS), the hydrophilic region of mouse heparanase (GenBank Accession No. AY077467), was synthesized and coupled with a terminal cysteine residue to keyhole limpet hemocyanin. This antigen was injected SC into rabbits, and antiserum was collected. Specific antibody to heparanase was purified with Affi-Gel 10 (Bio-Rad; Hercules, CA) coupled with the peptide.

Protein Extraction, SDS-PAGE, and Western Blotting

Lower molars from 3-week-old ICR mice were extracted, and the crown portion was then cut out using razor blades. Extraction of organic material was performed over a 24-hr period at a temperature of 4C using 4 M guanidine hydrochloride in 50 mM Tris-HCl buffer (pH 9.0) containing protease inhibitor cocktail (Sigma; St Louis, MO) and phosphatase inhibitor cocktail 2 (Sigma). The supernatant (tooth extract) was separated by centrifugation at 14,000 × g for 10 min, and the extract was dialyzed in PBS for 48 hr and concentrated with acetone. Precipitates were dissolved in 100 μl of sample buffer containing 4% SDS, 20% glycerol, and 5% mercaptoethanol in 100 mM Tris-HCl (pH 6.8).

SDS-PAGE was performed using 10% polyacrylamide gel. Sample was electrophoresed at 150 V for 75 min and then transferred to nitrocellulose membrane using 192 mM glycine and 20% methanol in 25 mM Tris–HCl (pH 8.3) at constant amperage of 50 mA for 40 min. The membrane was immersed in 10% skim milk in 10 mM Tris-buffered saline (TBS) for 30 min to block nonspecific binding and washed with TBS containing 0.05% Tween 20. The membrane was then incubated with rabbit anti-heparanase antibody (1 μg/ml) or rat anti-perlecan monoclonal antibody (Chemicon International; Temecula, CA) diluted 1:2000 for 12 hr at 4C, followed by incubation with horseradish peroxidase-conjugated anti-rabbit IgG (Sigma) or anti-rat IgG (Sigma) for 1 hr at room temperature. Immunoreactivity was visualized using ECL+ Western blotting detection reagents (Amersham Pharmacia Biotech; Buckinghamshire, England) according to the manufacturer's instructions.

Tissue Preparation for Histology

In this study, 1-, 2-, and 3-week-old ICR mice were used. Mice were anesthetized with sodium pentobarbital and perfused through the left ventricle with 4% paraformaldehyde and 0.1% glutaraldehyde in 0.05 M phosphate buffer (pH7.4) for light microscopy, or an acid–alcohol fixative composed of 96% ethanol, 1% glacial acetic acid, and 3% distilled water was used for perlecan immunohistochemistry (IHC) (Folkvord et al. 1989). Mandibles were dissected, immersed in the same fixative for 2 hr at 4C, and decalcified in 5% EDTA, pH 7.4, for 2 weeks at 4C.

For light microscopy, specimens were dehydrated in a graded ethanol series and embedded in paraffin. Four-μm-thick sections were cut, dewaxed with xylene, and stained with hematoxylin and eosin.

Perlecan and Laminin IHC

Sections were transferred to 5 mM periodic acid for 10 min at room temperature to block endogenous peroxidase and then immersed in PBS containing 10% BSA for 30 min. For IHC study of perlecan, sections were treated with 15,000 U/ml of hyaluronidase (Sigma) in PBS for 30 min at 37C. Localization of laminin was used to indicate basement membrane preservation in double immunofluorescence labeling. After washing in PBS, sections were incubated with an anti-laminin polyclonal antibody diluted 1:100 (Sigma) and an anti-perlecan monoclonal antibody diluted 1:200 (Chemicon) for 12 hr at 4C. For immunofluorescence, sections were incubated with Alexa Fluor-594 goat anti-rabbit IgG (diluted 1:200; Molecular Probes, Eugene OR) and Alexa Fluor-488 goat anti-rat IgG (Molecular Probes) diluted 1:200 for 1 hr at room temperature. Sections were then examined under an All-in-one Type Fluorescence Microscope (BZ-8000; Keyence, Osaka, Japan) using BZ Analyzer Software (Keyence).

Osteopontin, Bone Sialoprotein, and Cytokeratin IHC

Sections were treated with 0.1% trypsin (Sigma) in PBS for 15 min at room temperature. After washing in PBS, sections were incubated with an anti-cytokeratin monoclonal antibody (Nichirei; Tokyo, Japan) and an anti-osteopontin polyclonal antibody diluted 1:1000 (Nakamura et al. 1997) or an anti-bone sialoprotein polyclonal antibody diluted 1:500 (LSL; Tokyo, Japan) for 12 hr at 4C. For immunofluorescence, sections were incubated with Alexa Fluor-594 goat anti-rabbit IgG (Molecular Probes) diluted 1:200 and Alexa Fluor-488 goat anti-mouse IgG (Molecular Probes) diluted 1:200 for 1 hr at room temperature. Sections were then examined under the microscope (Keyence).

Heparanase IHC

For IHC study of heparanase, sections were transferred to 5 mM periodic acid for 10 min to block endogenous peroxidase. After blocking with 10% BSA for 30 min, they were incubated with an anti-heparanase polyclonal antibody (3 μg/ml) for 12 hr at 4C. Sections were then incubated with a secondary antibody (ChemMate ENVISION; Dako Cytomation, Carpinteria, CA) for 1 hr at room temperature. After washing with PBS, immunoreactivity was visualized by immersion in a DAB–H_2O_2 solution (0.05% DAB and 0.01% H_2O_2) in 0.05 M Tris–HCl buffer, pH 7.6) for 10 min at room temperature. Sections were then stained with hematoxylin, dehydrated, and observed under the microscope (Keyence).

Controls

Control sections were incubated with rat, mouse, and rabbit IgG preimmune serum or without a primary antibody.

Results

Western Blotting Analysis

Anti-heparanase antibody reacted with a 42-kDa band in the tooth extract (Figure 1A). No other band was detected with this antibody. Anti-perlecan antibody reacted with a broad band (>250 kDa) in the tooth extract, as well as with 130- and 115-kDa bands (Figure 1B).

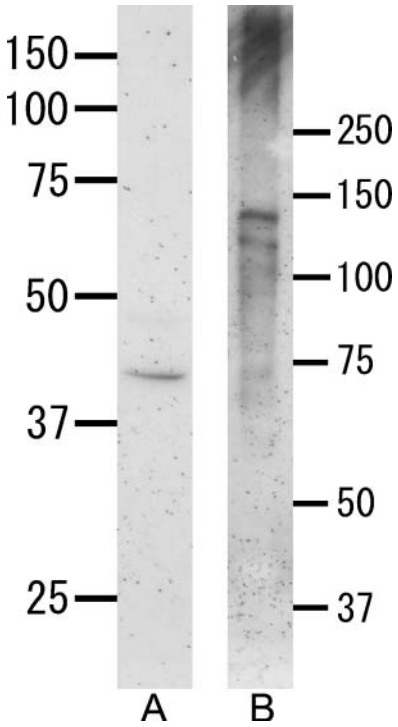

Figure 1 Western blotting with anti-heparanase antibody (**A**) or anti-perlecan antibody (**B**) under reduced conditions. (**A**) An intense band at 42 kDa is detected. (**B**) A broad band >250 kDa is seen in the tooth extract. Two bands are also visible at 130 kDa and 115 kDa.

Light Microscopy and Localization of Cytokeratin

At the initial stage of root formation, HERS was formed by inner and outer enamel epithelial cells (Figure 2A). During root formation, odontoblasts were aligned on the pulpal side of the root dentin. Cells separated from HERS were seen in the periodontal ligament (Figure 2B). Both acellular and cellular cementum were present on the dentin as root formation progressed (Figure 2C). Cementoblasts located on the cementum surface and cementocytes buried in the cementum matrix were also seen (Figure 2D). Epithelial rests of Malassez were seen among the periodontal ligament (Figure 2E).

Localization of Laminin and Perlecan

During root formation, the basement membrane surrounding HERS showed intense immunoreactivity for laminin (Figures 3A, 3C, and 3G). The basement membrane of epithelial rests of Malassez also showed laminin-positive labeling (Figure 3I). Discontinuous laminin reactivity was detected on the root surface (Figure 3E). Perlecan was present throughout the basement membrane at the initial stage of root formation (Figure 3B). With progressing root formation, perlecan labeling was scarce on the basement membrane facing the dental follicle, although it was visible at the tip of HERS (Figure 3D). At the late stage of root formation, weak immunoreactivity for perlecan was detected on the inner side of the basement membrane of HERS (Figure 3H). The root surface did not show perlecan-positive immunoreactivity (Figure 3F). The periodontal ligament and basement membrane of epithelial rests of Malassez exhibited positive immunoreactivity for perlecan (Figures 3H and 3J), and perlecan labeling was also detected in odontoblasts and predentin (Figure 3J).

No specific immunoreactivity was observed in the control sections incubated with rat and rabbit IgG or without primary antibody (data not shown).

Localization of Cytokeratin and Osteopontin or Bone Sialoprotein

At the late stage of root formation, cytokeratin-positive immunoreactivity was seen in the cells of HERS, cells of fragments of HERS, and epithelial rests of Malassez (Figures 4A and 4B). Strong osteopontin labeling was observed on cementum matrix of acellular and cellular cementum (Figure 4A). Very little immunoreactivity for bone sialoprotein was seen on acellular cementum matrix (Figure 4B). No colocalization of cytokeratin and osteopontin or bone sialoprotein was detected in the cells of HERS, cells of fragments of HERS, and epithelial rests of Malassez (Figures 4A and 4B).

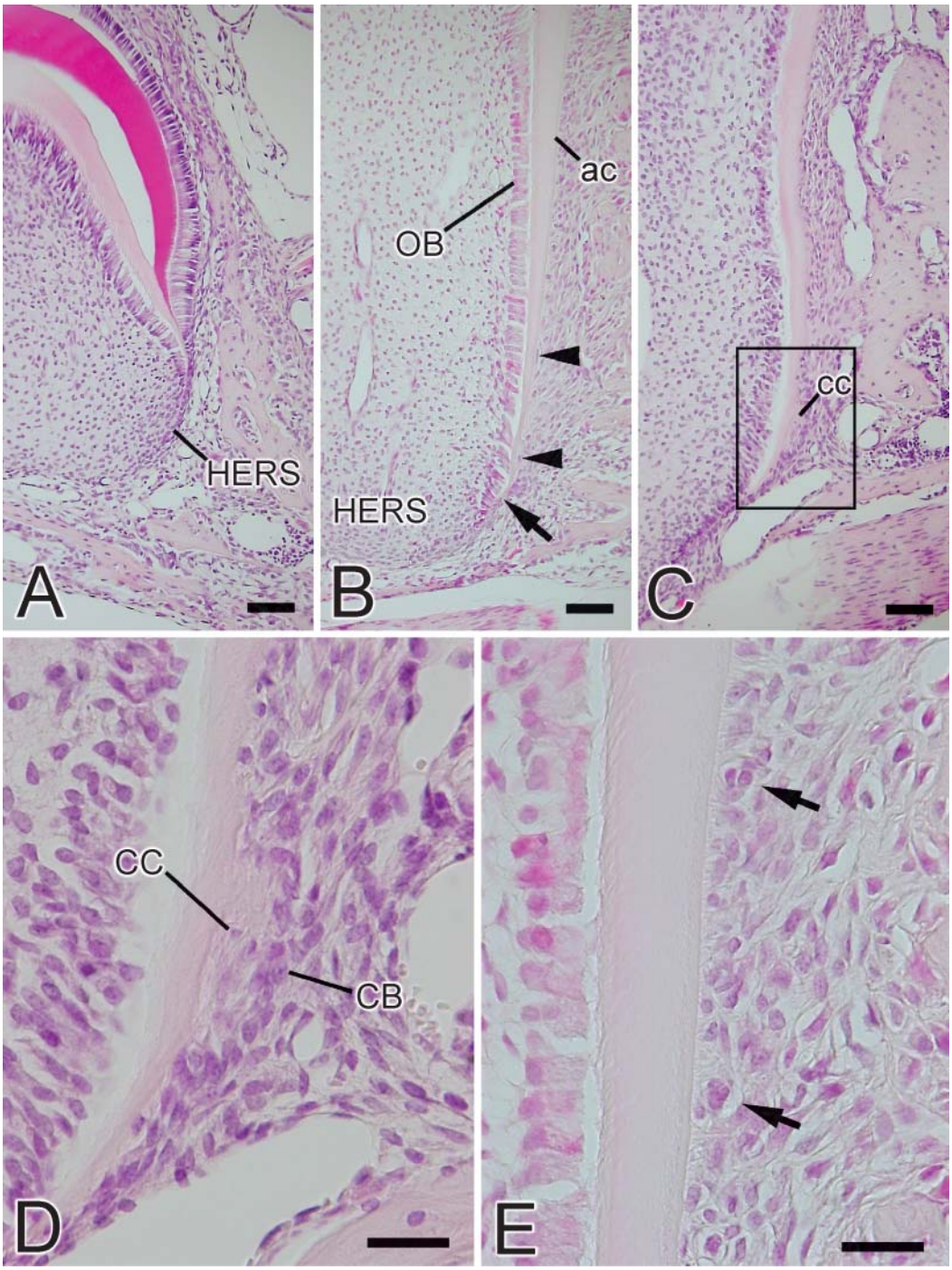

Figure 2 Light micrographs of the murine molar at the root-forming stage. (**A**) Third molar of a 2-week-old mouse. Hertwig's epithelial root sheath (HERS) consisting of inner and outer enamel epithelial cells is seen as the extension of the enamel organ. (**B**) First molar of a 2-week-old mouse at the advanced stage of root formation. HERS is observed at the apical end of the tooth root and loses its continuity (arrow). Several fragments of HERS are seen (arrowheads) facing acellular cementum (ac) surface. OB, odontoblasts. (**C**) First molar of a 3-week-old mouse. Cellular cementum (cc) is formed on the root dentin. (**D**) Higher magnification of the square in **C**. Cementoblasts (CB) and cementocytes (CC) are seen on the surface of the cementum and in cementum matrix, respectively. (**E**) Epithelial rests of Malassez are observed among the periodontal ligament (arrows). Bars: **A–C** = 50 μm; **D,E** = 20 μm.

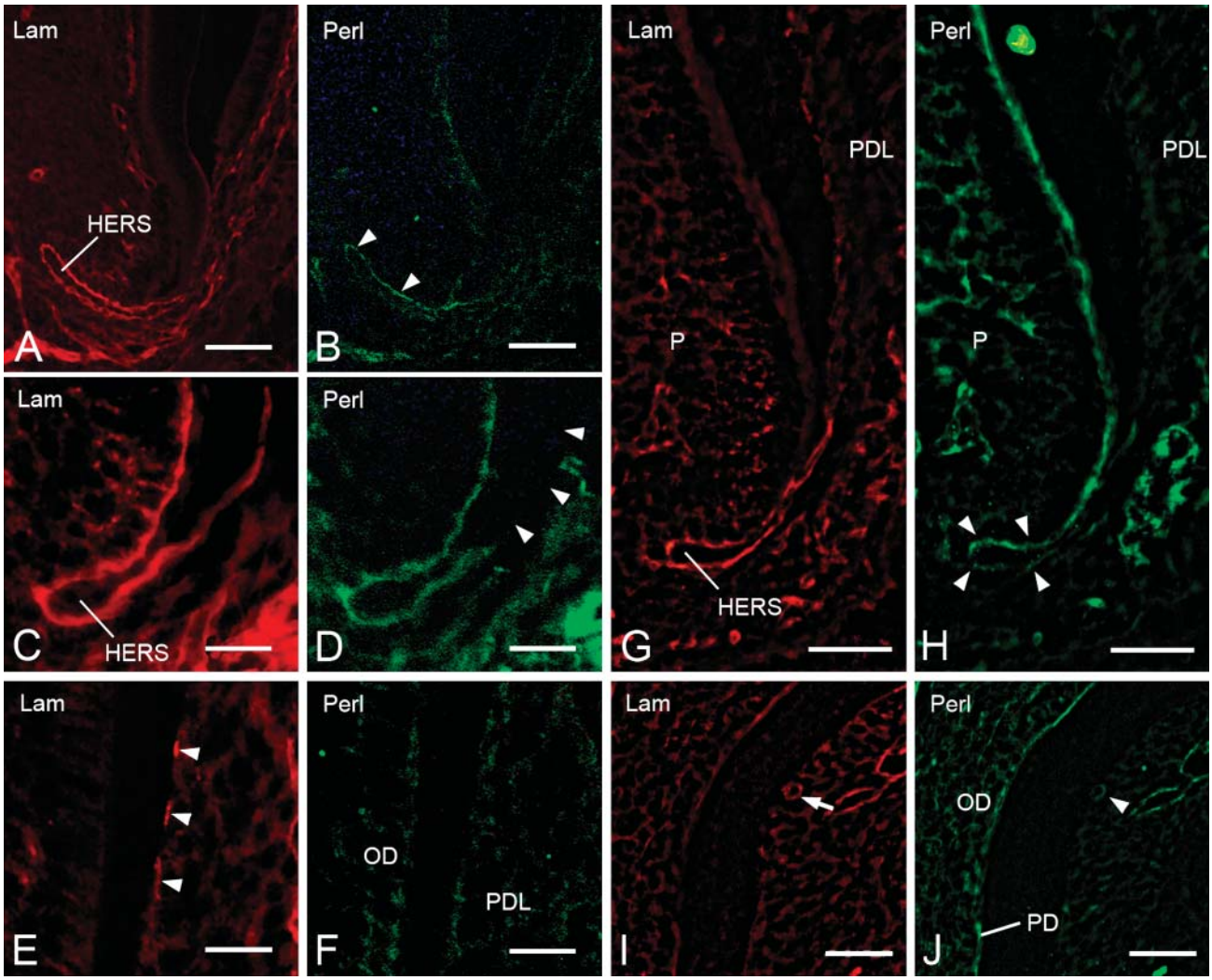

Figure 3 Fluorescent micrographs showing localization of laminin (**A,C,E,G,I**) and perlecan (**B,D,F,H,J**) on the basement membrane during tooth root formation. (**A,B**) Second molar of a 1-week-old mouse. Laminin and perlecan immunoreactivity are observed on the basement membrane of HERS. Intense reactivity for perlecan is detected on the inner side of HERS (arrowheads). Moderate immunoreactivity is seen on the outer side of HERS. (**C,D**) First molar of a 2-week-old mouse. Laminin labeling is seen throughout the basement membrane. Perlecan labeling is partially absent on the outer side (arrowheads). (**E,F**) First molar of a 2-week-old mouse. Regions are more cervical than those of Figures 4C and 4D. Discontinuous laminin immunoreactivity is detected on the root surface (arrowheads). No reactivity for perlecan is seen on the root surface. OD, odontoblasts; PDL, periodontal ligament. (**G,H**) First molar of a 3-week-old mouse. Laminin immunoreactivity is observed throughout the basement membrane. Weak perlecan reactivity is detected on the inner side of the basement membrane of HERS (arrowheads). P, pulp. (**I,J**) First molar of a 3-week-old mouse. Regions are more cervical than those of Figures 4G and 4H. Laminin labeling is seen around the cells of epithelial rests of Malassez (arrow). Weak perlecan reactivity is observed (arrowhead). Intense labeling for perlecan is seen in odontoblasts and predentin (PD). Bars: **A,B,G,H** = 50 μm; **C–F,I,J** = 25 μm.

Localization of Heparanase

At the initial stage of root formation, weak heparanase expression was detected in the cells of HERS (Figure 5A). During root development, intense heparanase immunoreactivity was detected in the cytoplasm of the inner and outer cells of HERS (Figures 5B–5D). Cells separated from HERS also showed heparanase-positive labeling (Figures 5B and 5E). At advanced stages of root development, immunoreactivity was detected in the cells of epithelial rests of Malassez (Figure 5C).

No specific immunoreactivity was detected in the control sections incubated without a primary antibody or with preimmune rabbit serum (data not shown).

Discussion

In this study we demonstrated localization of perlecan and heparanase during root formation in murine molars. The protein core of perlecan consists of five different domains, and the molecular mass of perlecan is reportedly

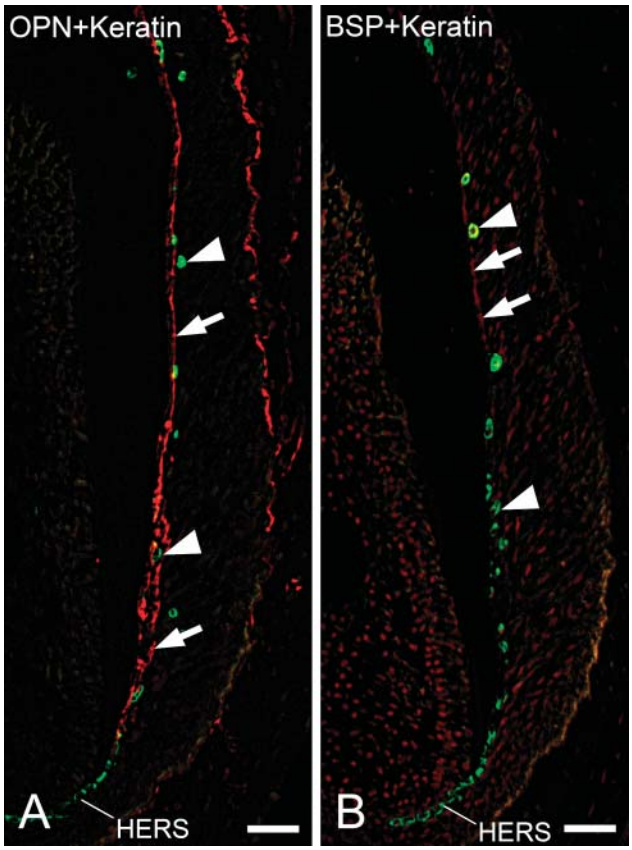

Figure 4 Fluorescent micrographs indicating localization of cytokeratin and osteopontin or bone sialoprotein at the late stage of root formation. (**A**) First molar of a 3-week-old mouse. Merged fluorescent micrograph indicating localization of cytokeratin (green) and osteopontin (red). HERS cells, fragment cells, and cells of epithelial rests of Malassez show cytokeratin-positive reactivity (arrows). Intense reactivity for osteopontin is detected on cementum matrix of acellular and cellular cementum (arrowheads). No colocalization of cytokeratin and osteopontin is seen in HERS cells, fragment cells, and cells of epithelial rests of Malassez. Adjacent section of Figure 4B. (**B**) First molar of a 3-week-old mouse. Merged fluorescent micrograph indicating localization of cytokeratin (green) and bone sialoprotein (red). Cytokeratin labeling is seen in HERS cells, some cells separated from HERS, and cells of epithelial rests of Malassez (arrows). Weak bone sialoprotein labeling is observed on the root surface (arrowheads). No colocalization of cytokeratin and bone sialoprotein is detected in HERS cells, fragments of HERS, and cells of epithelial rests of Malassez. Adjacent section of Figure 4A. Bar = 50 μm.

~400 kDa (Noonan et al. 1991). In present Western blotting analysis, perlecan was found in tooth extract as rather broad bands with a molecular mass >250 kDa. It is possible that the smaller molecular mass bands at 130 and 115 kDa visibly represented degradation products. Degradation occurs by multiple classes of enzymes that need to act coordinately. In addition to the action of heparanase on degrading glycosaminoglycan, the protein component of HSPG is cleaved by other enzymes. Thus, enzymes secreted from dental tissues such as matrix metalloproteinase and plasmin (Whitelock et al. 1996; Zhou et al. 1999; Winter et al. 2005) may be associated with perlecan degradation.

Western blotting analysis revealed that the peptide antibody for heparanase reacts with a 42 kDa band in tooth extract. This molecular mass is similar to the calculated mass of the larger fragment of mouse heparanase (43.2 kDa) (Miao et al. 2002).

As root formation progressed, perlecan disappeared first from the basement membrane facing the dental follicle. Perlecan was then scarce on the outer side of the basement membrane of HERS with the progression of root formation. Conversely, heparanase localized in the cells of HERS. Results of the present study suggest that heparanase is involved in the degradation of perlecan in the dental basement membrane.

We have demonstrated intense immunoreactivity for heparanase in the cells of HERS, suggesting that cells of HERS are involved in the degradation of basement membrane components by secreting heparanase during tooth morphogenesis. It is also feasible that heparanase-labeled cells could contribute to degradation of the HS chain present in periodontal ligament. Moreover, perlecan labeling was scarce on the basement membrane facing dental follicle with progressing root formation. This evidence suggests that perlecan degradation by heparanase derived from HERS is involved in rupture of HERS. Furthermore, intense immunoreactivity for heparanase was seen in cells that had separated from HERS. At the same stage, the inner basement membrane that had been in contact with the fragmented HERS was devoid of perlecan and HS (data not shown), despite the fact that it contained laminin and type IV collagen (data not shown). It is conceivable that heparanase-labeled fragment cells could participate in degradation of perlecan present in the separated basement membrane prior to degradation of laminin and type IV collagen.

It has been shown that all odontogenic epithelia are stained by the antibodies AE1 and AE3 (Sun et al. 1984). These antibodies have been used together to study immunolocalization of the tissue distribution of keratins, various diseases of the epidermis, the oral mucosa, and epithelial development, as well as to distinguish carcinoma from non-carcinoma (Sawaf et al. 1991). We also found colocalization for heparanase and cytokeratin in the HERS cells, fragment cells of the HERS, and cells of epithelial rests of Malassez, suggesting that cytokeratin-positive cells secrete heparanase during root formation.

According to the classical theory, the dental follicle proper, and perhaps also the perifollicular mesenchyme, give rise to periodontal ligament fibroblasts, osteoblasts, and cementoblasts (Ten Cate 1997; Cho and Garant 2000). Mature cementoblasts secrete initial cementum matrix on the root dentin. Osteopontin and bone sialoprotein, major non-collagenous proteins of cementum, are expressed by cementoblasts during early

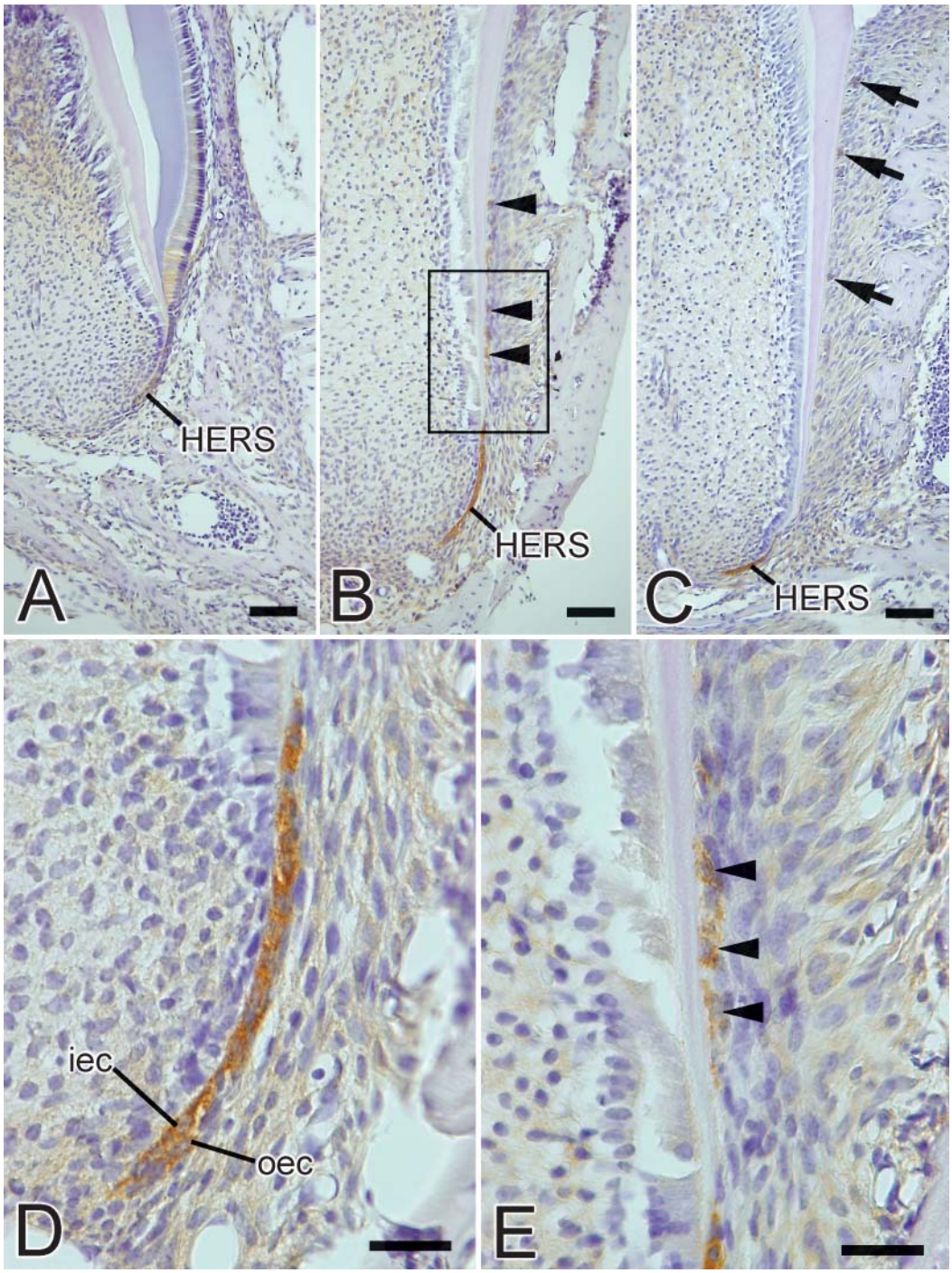

Figure 5 Light micrographs showing the localization of heparanase during tooth root formation. (**A**) Third molar of a 2-week-old mouse. Weak immunoreactivity for heparanase is visible in HERS cells. (**B**) First molar of a 2-week-old mouse. Intense immunoreactivity for heparanase is observed in cells of HERS. Fragments of HERS (arrowheads) also show heparanase-positive reactivity. (**C**) First molar of a 3-week-old mouse. Intense labeling is seen in the cells of HERS. Cells of epithelial rests of Malassez (arrows) show positive immunoreactivity. (**D**) Higher magnification of HERS. Immunoreactivity is seen in the cytoplasm of inner (iec) and outer (oec) enamel epithelial cells. (**E**) Higher magnification of square in **B**. Labeling is also detected in some cells separated from HERS (arrowheads). Bars: **A–C** = 50 μm; **D,E** = 20 μm.

stages of tooth root development (Bosshardt et al. 1998b). However, an alternative is that cells of HERS undergo an epithelial–mesenchymal transformation (Bosshardt and Nanci 1998a; Lezot et al 2000). We performed IHC studies to determine whether the cytokeratin-positive cells located in the periodontal ligament exhibit osteopontin and bone sialoprotein. We demonstrated immunolocalization of cytokeratin in the cells of HERS, cells of fragments of HERS, and epithelial rests of Malassez. However, immunoreactivity for osteopontin and bone sialoprotein was not detected in cytokeratin-positive cells. Therefore, we could not conclude that cells derived from HERS could acquire the cementoblast phenotype. Further research is needed to identify transforming cells and to determine the origin of cementoblasts.

Cleavage of HS chains by heparanase is known to induce cell growth and cell migration by releasing HS-binding cytokines and growth factors such as basic fibroblast growth factor (bFGF) (Ishai-Michaeli et al. 1990). It has also been shown that bFGF is released by biologically relevant enzymes such as plasmin, collagenase, and heparanase, which may have a role in the regulation of the growth factor activity (Whitelock et al. 1996). Perlecan has been shown specifically to bind bFGF, which binds to the HS on domain 1 of perlecan (Iozzo et al. 1994). Thus, perlecan is a potent modulator of cell growth. Using experimentally induced periodontal defects in beagle dogs, it has been demonstrated that bFGF accelerates healing of periodontal tissues, particularly cementum and periodontal ligaments (Murakami et al. 2003; Sato et al. 2004). In addition, it has been reported that bFGF is found predominantly within the dental basement membrane of HERS and the mesenchyme in early stages of tooth formation (Cam et al. 1992; Russo et al. 1998). These results suggest that bFGF may enhance proliferation and migration of dental follicular cells that develop into cementoblasts and periodontal ligament cells. In this study, perlecan disappeared from the basement membrane facing the dental follicle as root formation progressed, and heparanase was observed in the cells of HERS. Hence, heparin-binding growth factors such as FGF and TGFβ may be released from the HS chain by heparanase. Heparanase might be involved in the differentiation of cementoblasts by cleaving of HS chains of perlecan in the dental basement membrane, although eruption forces and mechanical stress are also important to cementoblast differentiation. The precise mechanism of cementoblast differentiation needs to be validated.

In conclusion, we provide the first evidence that perlecan disappears from the basement membrane of HERS and the fragmented HERS with the progression of root formation. In contrast to perlecan, heparanase localizes in the cells of HERS, the fragmented HERS, and the cells of epithelial rests of Malassez. Thus, our studies suggest that heparanase secreted by the cells of HERS contributes to root formation by degrading perlecan in the dental basement membrane.

Acknowledgments

This investigation was supported in part by a grant (No. 16791106) for scientific research from the Ministry of Education, Culture, Sports, Science and Technology of Japan.

We thank Dr. Noriyuki Nagaoka and Dr. Tomoko Yamamoto for technical support and special thanks to Dr. Takehito Tsuji for his support.

Literature Cited

Andujar MB, Magloire H, Hartmann DJ, Ville G, Grimaud JA (1985) Early mouse molar root development: cellular changes and distribution of fibronectin, laminin and type-IV collagen. Differentiation 30:111–122

Bosshardt DD, Nanci A (1998a) Immunolocalization of epithelial and mesenchymal matrix constituents in association with inner enamel epithelial cells. J Histochem Cytochem 46:135–142

Bosshardt DD, Schroeder HE (1996) Cementogenesis reviewed: a comparison between human premolars and rodent molars. Anat Rec 245:267–292

Bosshardt DD, Zalzal S, McKee MD, Nanci A (1998b) Developmental appearance and distribution of bone sialoprotein and osteopontin in human and rat cementum. Anat Rec 250:13–33

Cam Y, Neumann MR, Oliver L, Raulais D, Janet T, Ruch JV (1992) Immunolocalization of acidic and basic fibroblast growth factors during mouse odontogenesis. Int J Dev Biol 36:381–389

Cho MI, Garant PR (2000) Development and general structure of the periodontium. Periodontol 2000 24:9–27

Folkvord JM, Viders D, Coleman-Smith A, Clark RAF (1989) Optimization of immunohistochemical techniques to detect extracellular matrix proteins in fixed skin specimens. J Histochem Cytochem 37:105–113

Gallagher JT (2001) Heparan sulfate: growth control with a restricted sequence menu. J Clin Invest 108:357–361

Hassell JR, Robey PG, Barrach HJ, Wilczek J, Rennard SI, Martin GR (1980) Isolation of a heparan sulfate-containing proteoglycan from basement membrane. Proc Natl Acad Sci USA 77:4494–4498

Hulett MD, Freeman C, Hamdorf BJ, Baker RT, Harris MJ, Parish CR (1999) Cloning of mammalian heparanase, an important enzyme in tumor invasion and metastasis. Nat Med 5:803–809

Ida-Yonemochi H, Ohshiro K, Swelam W, Metwaly H, Saku T (2005) Perlecan, a basement membrane-type heparin sulfate proteoglycan, in the enamel organ: its intraepithelial localization in the stellate reticulum. J Histochem Cytochem 53:763–772

Iozzo RV, Cohen IR, Grassel S, Murdoch AD (1994) The biology of perlecan: the multifaceted heparan sulphate proteoglycan of basement membranes and pericellular matrices. Biochem J 302: 625–639

Ishai-Michaeli R, Eldor A, Vlodavsky I (1990) Heparanase activity expressed by platelets, neutrophils, and lymphoma cells releases active fibroblast growth factor from extracellular matrix. Cell Regul 1:833–842

Laurie GW, Leblond CP, Martin GR (1982) Localization of type IV collagen, laminin, heparan sulfate proteoglycan, and fibronectin to the basal lamina of basement membranes. J Cell Biol 95:340–344

Lezot F, Davideau JL, Thomas B, Sharpe P, Forest N, Berdal A (2000) Epithelial Dlx-2 homogene expression and cementogenesis. J Histochem Cytochem 48:277–284

MacNeil R, Thomas HF (1993) Development of the murine periodontium. I. Role of basement membrane in formation of a mineralized tissue on the developing root dentin surface. J Periodontol 64:95–102

Miao HQ, Navarro E, Patel S, Sargent D, Koo H, Wan H, Plata A, et al. (2002) Cloning, expression, and purification of mouse heparanase. Protein Expr Purif 26:425–431

Murakami S, Takayama S, Kitamura M, Shimabukuro Y, Yanagi K, Ikezawa K, Saho T, et al. (2003) Recombinant human basic fibroblast growth factor (bFGF) stimulates periodontal regeneration in class II furcation defects created in beagle dogs. J Periodontal Res 38:97–103

Nakamura H, Yamada M, Fukae M, Yanagisawa T, Ozawa H (1997) The localization of CD44 and moesin in osteoclasts after calcitonin administration in mouse tibiae. J Bone Miner Metab 15:184–192

Noonan DM, Fulle A, Valente P, Cai S, Horigans E, Sasaki M, Yamada Y, et al. (1991) The complete sequence of perlecan, a basement membrane heparin sulfate proteoglycan, reveals extensive similarity with laminin A chain, low density lipoprotein-receptor, and the neural cell adhesion molecule. J Biol Chem 266:22939–22947

Parish CR, Freeman C, Hulett MD (2001) Heparanase: a key enzyme involved in cell invasion. Biochim Biophys Acta 1471:M99–108

Russo LG, Maharajan P, Maharajan V (1998) Basic fibroblast growth factor (FGF-2) in mouse tooth morphogenesis. Growth Factors 15:125–133

Sato Y, Kikuchi M, Ohata N, Tamura M, Kuboki Y (2004) Enhanced cementum formation in experimentally induced cementum defects of the root surface with the application of recombinant basic fibroblast growth factor in collagen gel in vivo. J Periodontol 75:243–248

Sawaf MH, Ouhayoun JP, Forest N (1991) Cytokeratin profiles in oral epithelia: a review and a new classification. J Biol Buccale 19:187–198

Sun TT, Eichner R, Shermer A, Cooper D, Nelson WG, Weiss RG (1984) Classification, expression and possible mechanisms of evolution of mammalian epithelial keratins: a unifying model. The transformed phenotype. Cancer Cells 1:169–176

Ten Cate AR (1997) The development of the periodontium—a largely ectomesenchymally derived unit. Periodontol 2000 13:9–19

Thesleff I (2003) Epithelial-mesenchymal signalling regulating tooth morphogenesis. J Cell Sci 116:1647–1648

Thesleff I, Barrach HJ, Foidart JM, Vaheri A, Pratt RM, Martin GR (1981) Changes in the distribution of type IV collagen, laminin, proteoglycan, and fibronectin during mouse tooth development. Dev Biol 81:182–192

Tomazela-Herndl SA, Arana-Chavez VE (2001) Ultrastructure of early mineral deposition during hyaline layer formation in rat molars. Arch Oral Biol 46:305–311

Tomazela-Herndl SA, Arana-Chavez VE (2004) Localisation of sulphated glycoconjugates during hyaline layer formation in rat molars by ultrastructural cytochemistry. J Mol Histol 35:63–68

Toyoshima M, Nakajima M (1999) Human heparanase. Purification, characterization, cloning, and expression. J Biol Chem 274: 24153–24160

Vlodavsky I, Friedmann Y (2001) Molecular properties and involvement of heparanase in cancer metastasis and angiogenesis. J Clin Invest 108:341–347

Vlodavsky I, Friedmann Y, Elkin M, Aingorn H, Atzmon R, Ishai-Michaeli R, Bitan M, et al. (1999) Mammalian heparanase: gene cloning, expression and function in tumor progression and metastasis. Nat Med 5:793–802

Vlodavsky I, Goldshmidt O, Zcharia E, Atzmon R, Rangini-Guatta Z, Elkin M, Peretz T, et al. (2002) Mammalian heparanase: involvement in cancer metastasis, angiogenesis and normal development. Semin Cancer Biol 12:121–129

Whitelock JM, Murdoch AD, Iozzo RV, Underwood PA (1996) The degradation of human endothelial cell-derived perlecan and release of bound basic fibroblast growth factor by stromelysin, collagenase, plasmin, and heparanases. J Biol Chem 271: 10079–10086

Winter S, Kohl A, Huppertz A, Herold-Mende C, Wiest T, Komposch G, Tomakidi P (2005) Expression of mRNAs encoding for growth factors, ECM molecules, and MMP13 in mono-cultures and co-cultures of human periodontal ligament fibroblasts and alveolar bone cells. Cell Tissue Res 319:467–478

Zhou HM, Nichols A, Wohlwend A, Bolon I, Vassalli JD (1999) Extracellular proteolysis alters tooth development in transgenic mice expressing urokinase-type plasminogen activator in the enamel organ. Development 126:903–912

The Journal of Histochemistry & Cytochemistry